Chemical Papers (2019) 73:1469–1479
https://doi.org/10.1007/s11696-019-00698-w

ORIGINAL PAPER

A quinoline-based Schiff base for significant fluorescent "turn-on" and absorbance-ratiometric detection of Al^{3+}

Yu-Qing Ma[1] · Xue-Jiao Sun[1] · Ming-Qiang Li[1] · Shuang Zeng[1] · Zhi-Yong Xing[1] · Jin-Long Li[2]

Received: 28 August 2018 / Accepted: 28 January 2019 / Published online: 1 February 2019

Abstract

A novel quinoline-based Schiff base fluorescent sensor BQPA had been synthesized and characterized by common spectroscopic methods. It showed highly sensitive fluorescent enhancement (300-fold) and ratiometric absorbance for the determination of Al^{3+} with low detection limits of 31 nM in CH_3CH_2OH/H_2O (1: 9, v/v) solution. The stoichiometry of the BQPA–Al^{3+} complex was 1:1, determined by Job plots curve and further confirmed by HRMS, ^1H NMR titration and FT-IR spectrum. Moreover, the potential application of BQPA in the detection of Al^{3+} was estimated in real water samples.

Graphical abstract

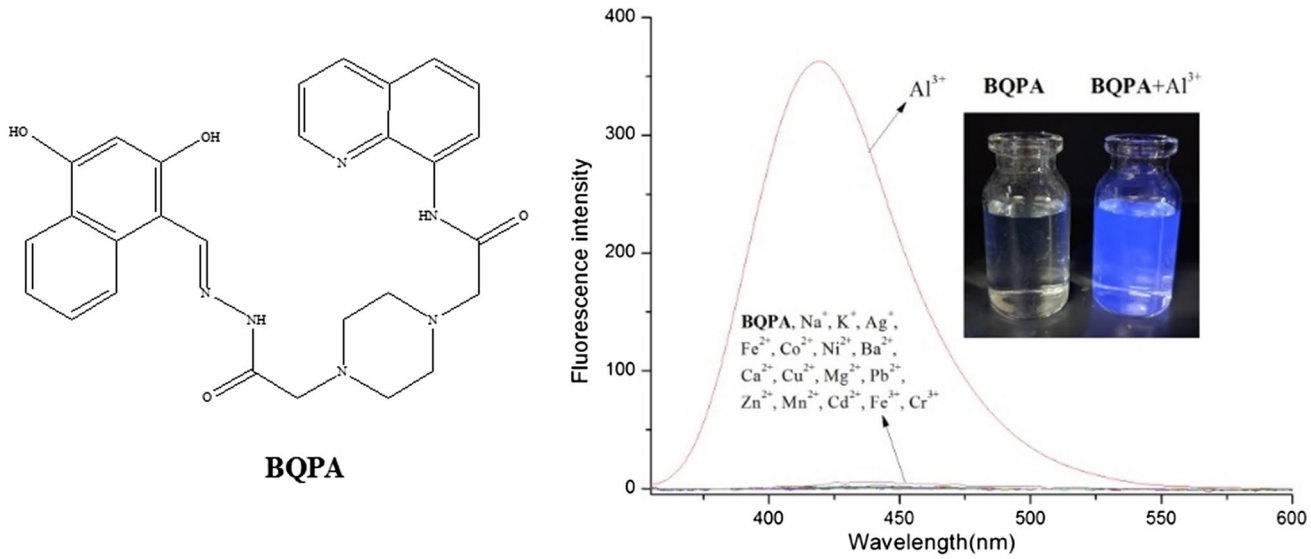

Keywords Quinoline · Schiff base · Fluorescence · Ratiometric · Al^{3+}

Introduction

The fluorescent method, due to its high selectivity and sensitivity, rapidity and convenient operation, has been employed in the detection of many kinds of analytes including various ions (Carter et al. 2014; Fu et al. 2019; Manjare et al. 2014; Öksüza et al. 2019; Özyol et al. 2018; Saçmaci et al. 2017), biothiols (Ren et al. 2018; Wang et al. 2018a, b), saccharide (Hosseinzadeh et al. 2015; Wang et al. 2015a, b) and protein

Electronic supplementary material The online version of this article (https://doi.org/10.1007/s11696-019-00698-w) contains supplementary material, which is available to authorized users.

✉ Zhi-Yong Xing
zyxing@neau.edu.cn

[1] Department of Applied Chemistry, College of Science, Northeast Agricultural University, Harbin 150030, People's Republic of China

[2] School of Chemistry and Chemical Engineering, Qiqihar University, Qiqihar 161006, People's Republic of China

(Chen et al. 2015; Huang et al. 2017). Aluminum, as the most abundant metal with its metallic forms in environment, has been widely used in human production activities including water treatment, package of food and medicines, and the production of light alloys (Kumawat et al. 2016; Shyamal et al. 2016). However, it is able to accumulate in environment and could affect human health through the biologic chain via water and organisms, and high levels of Al^{3+} may induce many physiological disorder and neurologic diseases, such as the Alzheimer's disease (AD), Parkinson's disease and so on (Good et al. 1992; Okem et al. 2015; Walton 2007). Moreover, the limit of concentration of Al^{3+} defined by the World Health Organization (WHO) in drinking water is 7.41 μM (Han et al. 2012). Hence, it is essential to develop highly selective and sensitive chemosensors for detecting the concentration of Al^{3+}, to protect the ecological environment and health.

Over the past few decades, many researchers had put their best efforts into developing chemosensors for metal ions, and a lot of Al^{3+} chemosensors had been reported (Balakrishnan et al. 2017; Dai et al. 2018; Gan et al. 2017; Kang et al. 2016; Lim et al. 2018; Maniyazagan et al. 2018; Singh et al. 2017; Wang et al. 2017a, b, 2018a, b, c; Yıldız et al. 2017; Zeng et al. 2018; Zhang et al. 2018; Zhu et al. 2016). However, there are some obstacles to designing an excellent fluorescent chemosensor for Al^{3+}. One is that Al^{3+} has drawbacks in its weak ability in coordination and strong ability in hydration; the other is that many reported probes suffer from shortcomings including multi-steps synthesis, being disturbed by other trivalent metal ions (Fe^{3+} and Cr^{3+}) and insolubility in water which further limits their practical applicability in real samples. More importantly, compared with the fluorescent turn-on (off) probes, the development of ratiometric probe is more appealing because it can eliminate the interference caused by the physical or chemical method through the ratio of two intensities of absorption or emission wavelength (Gupta et al. 2017; Manna et al. 2017; Naskar et al. 2018; Qin and Yang 2015a, b). Hence, the development of ratiometric probes for Al^{3+} is of great importance for the application in complex samples.

Quinoline-based derivatives have proved to be a popular fluorophore in construction chemosensors due to their structural diversity, favorable photophysical properties and potent binding affinities to many metal ions (Li et al. 2016; Qin and Yang 2015a, b; Roy and Rajak 2017; Singh et al. 2018; Wang et al. 2015a, b). However, only a few of them are ratiometric probes for the detection of Al^{3+} (Roy et al. 2016; Zhu et al. 2016). In addition, Al^{3+}, as a hard acid, prefers a hard-base coordination sphere containing N and O as the binding site (Fan et al. 2014). Taking the above statements into consideration, we designed a novel quinoline-based fluorescent probe *N′*-(2, 4-dihydroxybenzylidene)-2-(4-(2-oxo-2-(quinolin-8-ylamino)ethyl) piperazin-1-yl)acetohydrazide (BQPA), which showed a significant fluorescence turn-on (300-fold) and ratiometric absorbance for the determination of Al^{3+} in ethanol–water (1: 9, v/v) medium. Furthermore, BQPA was evaluated for the detection of Al^3 in real samples.

Experimental

Materials

All chemicals and reagents were purchased from commercial sources. The fluorescent spectra were recorded at room temperature on a Perkin Elmer LS55 fluorescence spectrometer. UV–Vis absorption spectra were obtained using a Pgeneral TU-1901 UV–Vis spectrophotometer. ^{1}H NMR and ^{13}C NMR spectra wererecorded on a Bruk AV-600 spectrometer, respectively. Mass spectra were measured on a Waters Xevo UPLC/G2-SQ Tof MS spectrometer.

Preparation of stock solution

A stock solution of BQPA (10 μM) was prepared with the solution of ethanol–water (1: 9, v/v).

Stock solutions (10 mM) of the cationic salts (Na^+, K^+, Ca^{2+}, Mg^{2+}, Ba^{2+}, Cr^{3+}, Mn^{2+}, Fe^{2+}, Fe^{3+}, Cu^{2+}, Ag^+, Co^{2+}, Ni^{2+}, Zn^{2+}, Cd^{2+}, Al^{3+} and Pb^{2+}) were prepared with ultrapure water, respectively. For spectrum measurement, the test solutions were prepared by adding a certain amount of stock solution using a pipette into the BQPA stock solution. During the measurement of fluorescent spectrum, the excitation was set at 350 nm, emission wavelength was recorded in the range of 300–600 nm, and emission intensity was recorded at 420 nm for the fluorescence titration, competitive experiments and Job's plot. The excitation and emission slit widths were 10 nm and 10 nm, respectively.

Al^{3+} standard solution (10 mM) was prepared by dissolving $Al(NO_3)_3{\cdot}9H_2O$ (0.5 mmol) in ultrapure water (50 mL).

Fluorescence and colorimetric measurements

$Al(NO_3)_3{\cdot}9H_2O$ (0.5 mmol) was dissolved in ultrapure water (50 mL). 2–50 μL of the Al^{3+} solution (10 mM) was transferred to BQPA solution (10 μM) prepared above, respectively. After mixing them for a few seconds, fluorescence spectra and UV–Vis absorption spectra were taken at room temperature, respectively. The color changes of BQPA (10 μM) were obtained in the presence of Al^{3+} ions (5 equiv.) in ethanol–water (1:9, v/v) under UV light of 365 nm.

Determination of binding constant and detection limit

According to the fluorescence intensity data, the binding constant of BQPA with Al^{3+} was calculated based on the modified Benesi–Hildebrand equation (Kadar et al. 2005), where, $F_{max,}$ F and F_{min} are the fluorescence intensities of BQPA in the presence of Al^{3+} at saturation, at an intermediate Al^{3+} concentration, and absence of Al^{3+}, respectively. K is the stability constant.

$$\frac{1}{F-F_{min}}=\frac{1}{K(F_{max}-F_{min})[Al^{3+}]}-\frac{1}{F_{max}-F_{min}}. \quad (1)$$

The limit of detection (LOD) of Al^{3+} was calculated on the basis of $3\sigma/S$ according to the fluorescence changes, where σ is the standard deviation of the blank solution and S is the slope of the calibration curve (Liu et al. 2016).

The limit of quantification (LOQ) of Al^{3+} was calculated on the basis of 10 σ/S according to the fluorescence changes, where σ is the standard deviation of the blank solution and S is the slope of the calibration curve (Chitnis and Akhlaghi 2008).

The quantification limit for Al^{3+} in water samples was spiked with standard Al^{3+} ions at different concentration levels, then diluted within working linear range, and analyzed with the method proposed under optimized conditions.

NMR titration

In three NMR tubes, BQPA (5 mg) dissolved in DMSO (0.5 mL) was added. Then different equivalents (0, 0.5 and 1 equiv.) of $Al(NO_3)_3$ in DMSO (0.5 mL) were added separately to the corresponding tube, and ^1H NMR spectra were measured in turn at room temperature.

Synthesis of compound BQPA

Compound BQPA was synthesized according to the synthetic route outlined in Scheme 1. The intermediate compounds **1–4** were prepared by the reported literature (Shao 2010; Wang et al. 2017a, b; Li et al. 2018).

A mixture of compound **4** (102 mg, 0.3 mmol) and 2, 4-hydroxybenzaldehyde (0.4 mmol) dissolved in ethanol (20 mL) was refluxed for 2 h (monitored by TLC) and then cooled to room temperature. The solvent was removed under reduced pressure, and the crude substance was further purified by column chromatography using CH_3OH /CH_2Cl_2 (v/v, 1/30) as eluent to get light yellow crystal BQPA (30 mg, 0.06 mmol), yield: 21.6%, m.p: 290–292 °C. ^1H NMR (600 MHz, DMSO-d_6) (Fig. S1): δ (ppm) 11.41 (s, 1H), 11.38 (s, 1H), 11.28 (s, 1H), 9.94 (s, 1H), 8.95 (m, 1H), 8.65 (dd, $J_1=7.2$ Hz, $J_2=1.2$ Hz, 1H), 8.41 (m, 2H), 7.67(d, $J=7.8$ Hz, 1H), 7.58–7.62 (m, 2H), 7.26 (d, J = 8.4 Hz, 1H), 6.31–6.36 (m, 2H), 3.34 (s, 2H), 3.19 (s, 2H), 2.69 (s, 8H). ^{13}C NMR (151 MHz, DMSO-d_6) (Fig. S2): δ (ppm)

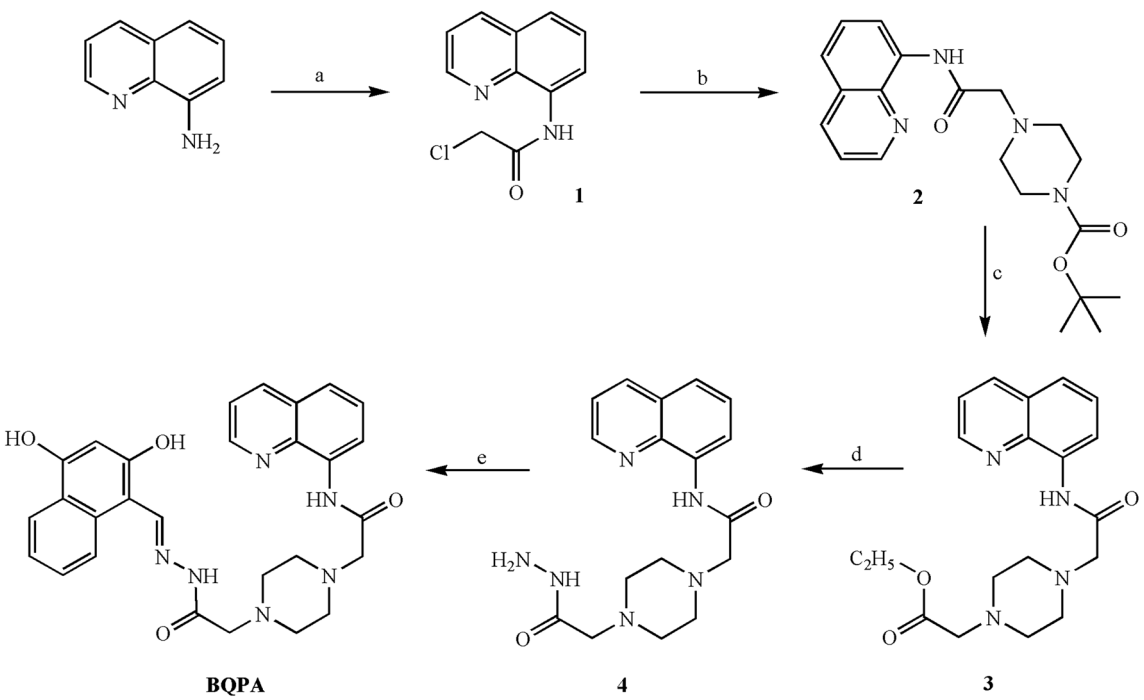

Scheme 1 The synthetic route of BQPA

169.11, 165.44, 161.34, 160.00, 149.72, 149.24, 138.49, 137.15, 134.61, 131.93, 128.44, 127.59, 122.76, 122.04, 115.94, 110.65, 107.97, 102.89, 62.25, 60.66, 53.38, 52.92. HRMS *m/z* (TOF MS ES$^+$) (Fig. S3): calcd for $C_{24}H_{27}N_6O_4$: 463.2094 $[M+H]^+$, found: 463.2097.

Results and discussion

Fluorescence spectra response of BQPA to ions

The selectivity of BQPA to various metal ions was examined in ethanol/water (1: 9, v/v). As shown in Fig. 1, there was almost no change in the fluorescence spectrum between the free BQPA and the mixture of BQPA with the tested metal ions (Na^+, K^+, Ca^{2+}, Mg^{2+}, Ba^{2+}, Cr^{3+}, Mn^{2+}, Fe^{2+}, Fe^{3+}, Cu^{2+}, Ag^+, Co^{2+}, Ni^{2+}, Zn^{2+}, Cd^{2+} and Pb^{2+}). However, a significant enhancement (300-fold) in fluorescence intensity was observed upon the addition of Al^{3+} centered at 420 nm, and the color of the BQPA solution changed from colorless into blue under the irradiation of 365 nm UV-lamp. This result could be attributed to the inhibition of the C=N bond rotation and chelation-enhanced fluorescence (CHEF) (Nie et al. 2017; Pang et al. 2018).

To further investigate the binding property of probe BQPA, fluorescence titration of probe BQPA with Al^{3+} was performed (Fig. 2). Upon excitation at 350 nm, probe BQPA alone exhibited a negligible emission at 420 nm. However, with the addition of Al^{3+} (0–5.0 equiv.) to a solution of probe BQPA in ethanol/water (1:9, v/v), a gradual increase in emission intensity of BQPA at 420 nm was observed and then almost reached a plateau when the addition of Al^{3+} was 20 μM (2 equiv.), indicating a stable complex formation between the probe BQPA and

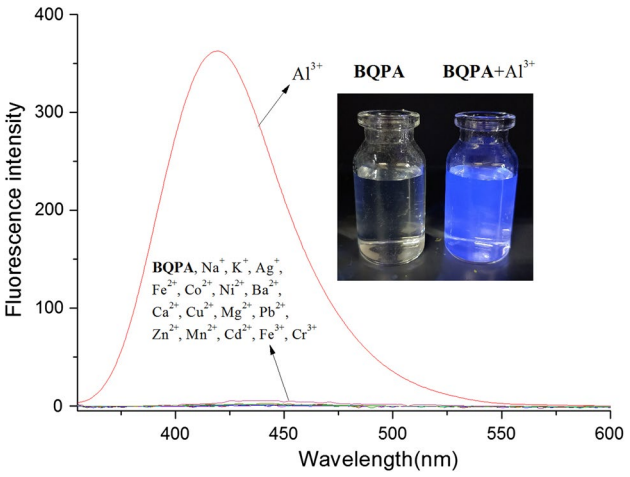

Fig. 1 Fluorescence spectra of BQPA (10 μM) with different metal ions (50 μM) in ethanol/water (1:9, v/v)

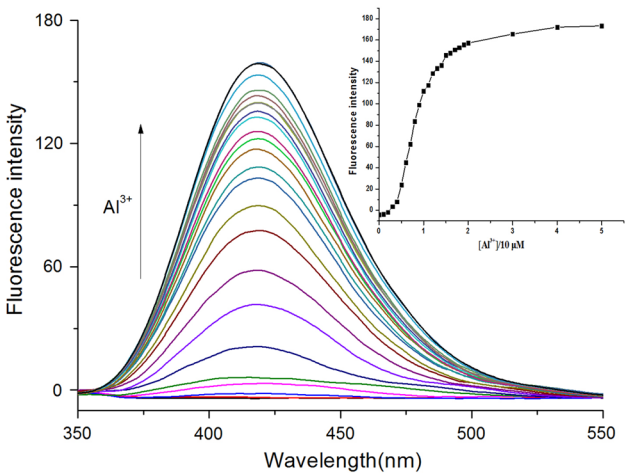

Fig. 2 Fluorescence emission spectra of BQPA in ethanol/water (1: 9, v/v) solution upon the addition of Al^{3+} (0–5.0 equiv.) with an excitation of 350 nm. Inset shows the fluorescence change at 420 nm with the addition of Al^{3+}

Al^{3+} (Wen and Fan 2016). Moreover, the maximal emission intensity of BQPA and the concentration of Al^{3+} (varying from 2 to 12 μM) showed a good linear relationship ($y = 143.0x - 37.0578$) (Fig. S4), and the detection limit of BQPA for Al^{3+} was calculated as 4.15×10^{-8} M (41.5 nM) (Liu et al. 2016), which met the requirement defined by the US Environmental Protection Agency (maximum allowed contamination of Al^{3+} is 7.4 μM in drinking water) (Han et al. 2012). Moreover, the limit of quantification (LOQ) of BQPA for Al^{3+} was calculated as 1.38×10^{-7} M (0.138 μM). These results indicated that BQPA could be used for the detection of Al^{3+} in drinking water.

To further visualize the fluorescence color changes with the addition of Al^{3+} to BQPA, we drew coordinates of BQPA and the BQPA–Al^{3+} complexes in the CIE diagram, as shown in Fig. 3. Upon the addition of various concentrations Al^{3+}, the coordinate changed from (0.25, 0.34) to (0.16, 0.04), which indicated the change of color from light blue to dark blue.

To investigate the anti-interference from the co-existing metals during the detection of Al^{3+}, competitive experiments in the presence of other metal ions (Na^+, K^+, Ca^{2+}, Mg^{2+}, Ba^{2+}, Cr^{3+}, Mn^{2+}, Fe^{2+}, Fe^{3+}, Cu^{2+}, Ag^+, Co^{2+}, Ni^{2+}, Zn^{2+}, Cd^{2+} and Pb^{2+}) were conducted. As shown in Fig. 4, the fluorescence intensity of the BQPA–Al^{3+} complex had no obvious variation upon the addition of competitive metal ions except Cu^{2+}, which caused the fluorescence of the BQPA–Al^{3+} complex to be completely quenched due to its paramagnetic property reported by other researchers (More and Shankarling 2017).

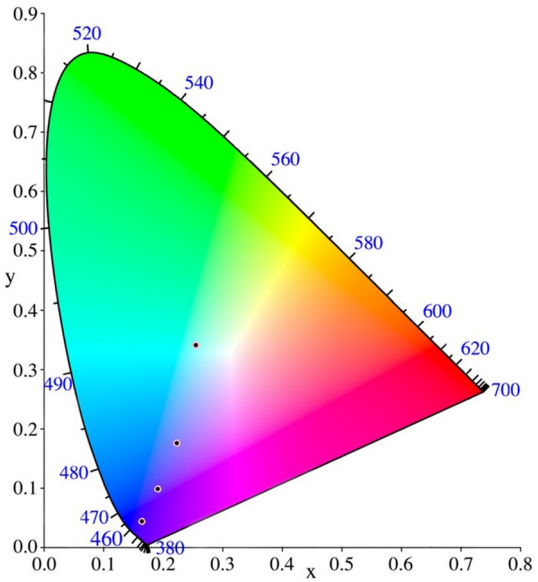

Fig. 3 The distribution of BQPA and BQPA with different equiv. Al^{3+} (0.1, 0.5, 5.0) in CIE

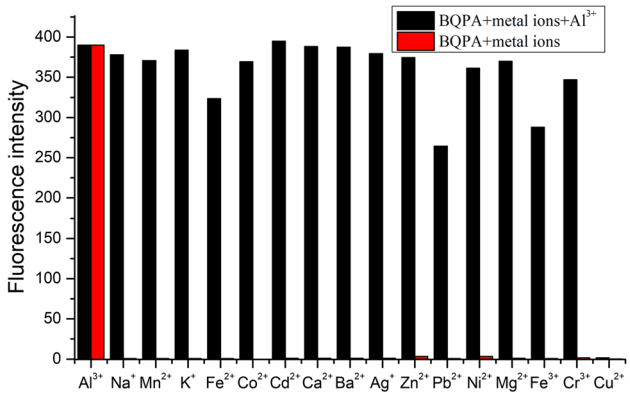

Fig. 4 Competitive selectivity of compound BQPA toward Al^{3+} over other metal ions (5 equiv.) in ethanol/water (1: 9, v/v)

UV–Vis response of BQPA toward Al^{3+}

According to the specific fluorescence responses of BQPA to Al^{3+} among the tested cations, the UV–Vis spectrum of BQPA (10 μM) were measured in the absence and presence of Al^{3+} (50 μM) in ethanol/H_2O (1/9, v/v) solution, respectively (Fig. 5). BQPA alone showed the maximum absorption centered at 295 nm and 317 nm, respectively. Importantly, a significant redshift (from 295 to 305 nm) was observed upon the addition of Al^{3+}. This result could be attributed to the enhancement of the conjugate system after the complexation of BQPA with Al^{3+} (Zhou et al. 2018).

Moreover, UV–Vis titration experiments were further carried out to investigate the binding properties of BQPA with Al^{3+} (Fig. 6). On gradual addition of Al^{3+} (0–2 equiv.) to the

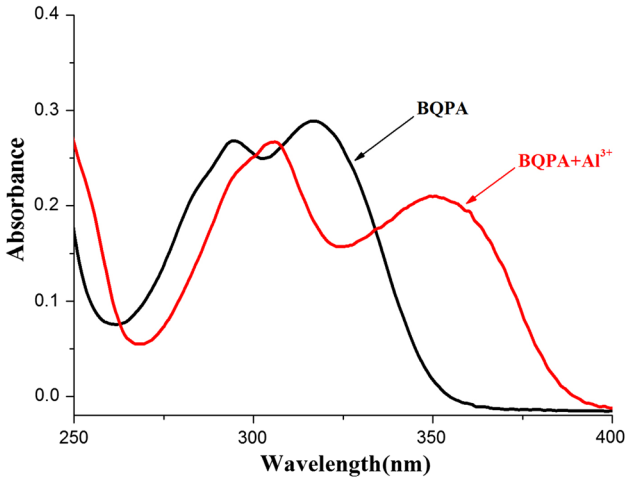

Fig. 5 UV–Vis absorption spectra of BQPA (10 μM) in the absence (black curve) and presence (red curve) of 5 equiv. of Al^3 in ethanol/water (1: 9, v/v)

solution of BQPA (Fig. 6a), an isosbestic point at 304 nm was observed, indicating the formation of the BQPA–Al^{3+} adduct. In addition, the absorbance intensity ratios of the BQPA at 317 nm and 295 nm (A_{317}/A_{295}) decreased gradually on the addition of Al^{3+} (Fig. 6b), and a good linear relationship ($y = -0.2858 + 1.1745$) could be seen between the absorbance intensity ratios (A_{317}/A_{295}) and the amount of Al^{3+} in the range of 4–9 μM (Fig. S5), indicating the practicability of the probe BQPA with the ability of ratiometric absorbance detection toward Al^{3+}. The detection limit and quantification limit were calculated to be as low as 31 nM and 103 nM, respectively, which were lower than the ones calculated above based on fluorescence titration. According to the above results, as for the probe BQPA, the ratiometric absorbance detection was more sensitivity than that by fluorescence intensity in the detection of Al^{3+}.

Analysis sensing mechanism of BQPA for Al^{3+}

Confirmation of binding stoichiometry

To determine the binding stoichiometry of BQPA with Al^{3+}, both mole–ratio plot and Job's plot were measured. According to the results of fluorescence titration (Fig. 2, insert) and UV–Vis titration (Fig. 6b) of probe BQPA with Al^{3+}, both the fluorescence intensity and absorbance ratios (A_{317}/A_{295}) almost remained constant when the addition of Al^{3+} was less than 1.5 equiv., which could be used as a preliminary proof for the 1:1 stoichiometry between BQPA and Al^{3+}. Moreover, the 1:1 binding stoichiometry was further identified by the Job's plot on the basis of its fluorescence intensity at 420 nm (Fig. 7). The maximum fluorescence intensity was seen when the mole fraction

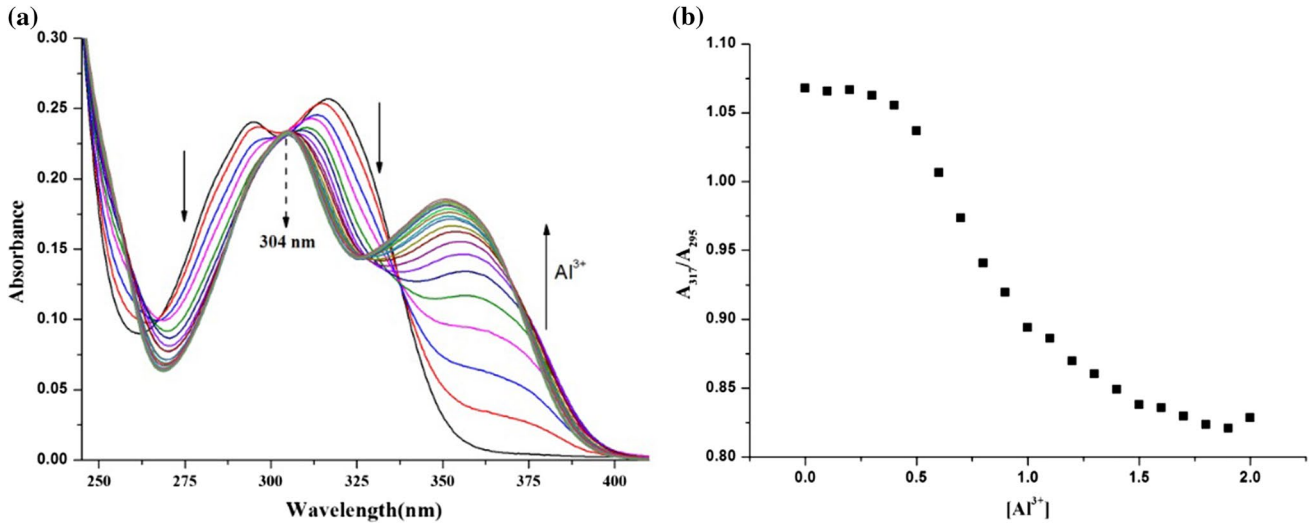

Fig. 6 **a** UV–Vis absorption spectra of BQPA (10 μM) in ethanol/water (1:9, v/v) upon the addition of Al^{3+} (0–2 equiv.); **b** the scatter plot of absorbance ratios (A_{317}/A_{295}) and Al^{3+} concentration

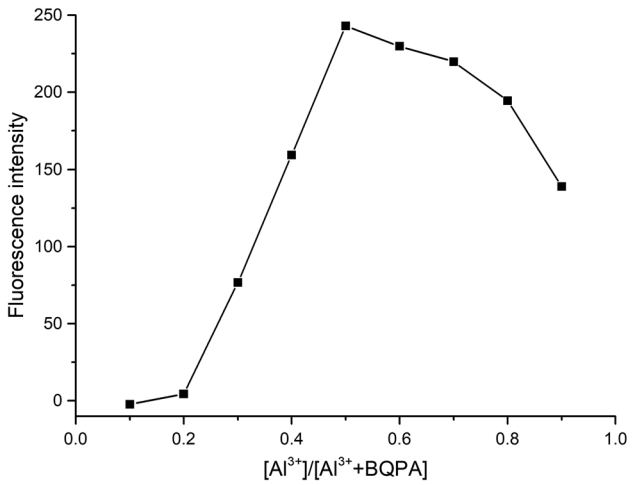

Fig. 7 Job's plot for determining the stoichiometry between BQPA and Al^{3+} ethanol/water (1:9, v/v) solution; the total concentration of BQPA and Al^{3+} was 10 μM)

of Al^{3+} was around 0.5, confirming a 1:1 stoichiometry for BQPA–Al^{3+} complexes in ethanol/water (1:9, v/v) solution.

Furthermore, HRMS of BQPA in the presence of Al^{3+} was measured and the result is shown in Fig. 8. The peaks at 487.1680 were attributed to $[BQPA-2H^{+}+Al^{3+}]^{+}$ (Calcd. *m*/*z* 487.1674), which was another credible evidence for the 1:1 binding stoichiometry of BQPA with Al^{3+} resulting from Job's plot analysis. So, the association constant of BQPA and Al^{3+} was calculated as 7.48×10^{5} M^{-1} (Fig. S6) according to the nonlinear curve fitting of the absorbance titration data, which is higher than the calculated 7.4×10^{4} M^{-1} based on the fluorescence titration data (Fig. S7).

H NMR titration

To get insight into the exact binding mode of BQPA–Al^{3+}, ^{1}H NMR titration experiments were measured in DMSO-d_6. As shown in Fig. 9, on addition of Al^{3+}, the protons of hydroxyl (H_b) and amide (H_d) groups of BQPA disappeared, indicating deprotonation during the process of coordination of Al^{3+} with the oxygen atom of the hydroxyl and the nitrogen atom of amide. Moreover, the protons of methylene (H_e and H_h) and the protons (H_f and H_g) of the piperazine ring of BQPA were all significantly shifted downfield to 3.49 ppm, indicating that the two nitrogen atoms acted as the binding sites involved in the coordination with Al^{3+}.

FT-IR measurement

To obtain more details for the binding site of BQPA with Al^{3+}, the FT-IR spectra of free BQPA and complex BQPA–Al^{3+} were measured (Fig. S8). BQPA exhibited strong absorbance at 3260 cm^{-1} and 3240 cm^{-1}, assignable to the stretching vibration of –OH and –NH, respectively. However, all of them disappeared in the spectra of complex BQPA–Al^{3+}, and two wide peaks at 3371 cm^{-1} and 3146 cm^{-1} indicated the –OH and –NH stretching vibrations, respectively. Moreover, the peaks at 1686 cm^{-1} and 1506 cm^{-1}, which belonged to the C=O and C–N stretching vibration of BQPA, shifted to the 1594 cm^{-1} and 1373 cm^{-1}, respectively. The above results indicated the coordination of BQPA with Al^{3+}. In addition, the comparison of probe BQPA with the reported chemosensors is summarized in Table 1. Compared with the reported probes, the advantages of probe BQPA was its lower detection limit (nM level) and high sensitivity through fluorescent signal response

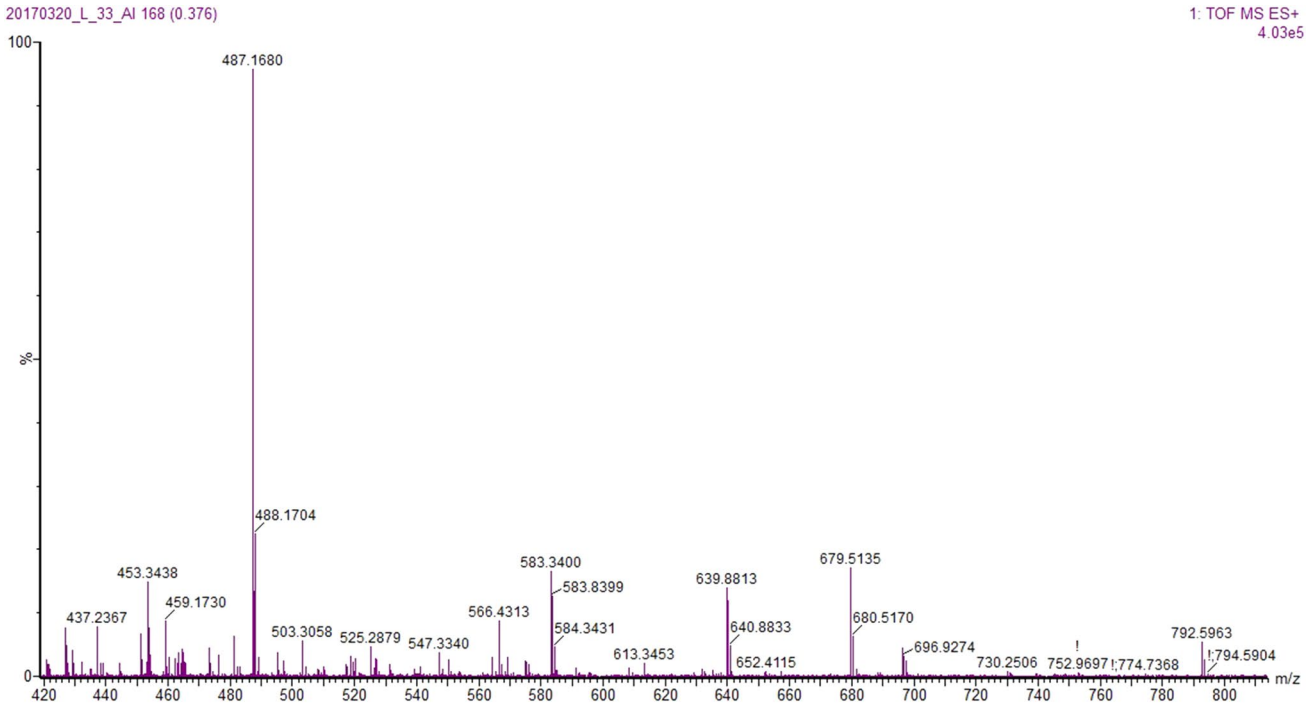

Fig. 8 ESI-MS spectrum of BQPA (50 μM) on addition of 5 equiv. of Al^{3+} in CH_3CH_2OH

(300-fold), but its insolubility in neat water was its shortcoming, which might to some extent limit its application in environment and in vivo.

Hence, according to the analysis of the experimental results mentioned above, a feasible bonding mode between BQPA and Al^{3+} was proposed (Scheme 2).

The effect of pH on the fluorescence of BQPA

The effect of pH ranging from 2.0 to 12.0 on the emission intensity ($\lambda_{em} = 420$ nm) of BQPA in the absence and presence of Al^{3+} was investigated (Fig. 10). The probe BQPA had almost no fluorescence emission in the wide pH range 2.0–12.0, but upon addition of Al^{3+} into BQPA at different pH conditions, obvious fluorescence enhancement was observed from pH 4–6, indicating that BQPA could be a good probe for Al^{3+} detection in acidic medium.

To understand the effect of pH on the detection of BQPA for Al^{3+} in acidic conditions, we detected the variation of pH with increase in the concentration of Al^{3+}, and the results were recorded by the double coordinate graph according to the fluorescence intensity ($\lambda_{em} = 420$ nm) and pH with various concentrations of Al^{3+} in ethanol–water (1:9, v/v) (Fig. 11). Within the 0–1.0 equiv. of Al^{3+} content, both pH and fluorescence intensity ($\lambda_{em} = 420$ nm) had good linear relationship with the concentration of Al^{3+}, which indicated that BQPA could detect Al^{3+} qualitatively and quantitatively by pH and fluorescence intensity under acidic conditions.

Reversibility of BQPA for Al^{3+}

To evaluate its practical application, the reversibility of BQPA was necessarily investigated in ethanol/water (1:9, v/v) solution by adding Na_2EDTA, which is a good chelating agent, to Al^{3+}. On addition of Al^{3+} to the solution of BQPA, both the UV–Vis absorption spectra (Fig. S9) and fluorescence spectra (Fig. S10) showed significant changes compared with the corresponding spectrum of BQPA itself. However, after addition of EDTA to the solutions of BQPA–Al^{3+}, the UV–Vis absorption spectra and fluorescence spectra of the solution of BQPA–Al^{3+} showed much more similarity to that of BQPA in the absence of Al^{3+}, indicating the recovery of BQPA. This result was also supported by the bonding constant of BQPA with Al^{3+} calculated as $7.4 \times 10^4\ M^{-1,}$ which was far lower than that of EDTA with Al^{3+} calculated as $1.99 \times 10^{16}\ M^{-1}$.

Application of BQPA to water samples

To explore the practical application of BQPA for the detection of aluminum ions, detailed experiments were carried out for the determination of Al^{3+} in real water samples collected from our university campus (Table 2). The results showed that BQPA had high accuracy for the practical application of aluminum ions in water. In addition, to investigate about the co-existence of Cu^{2+} during the detection of Al^{3+} in real water samples, different concentrations of Cu^{2+} were added

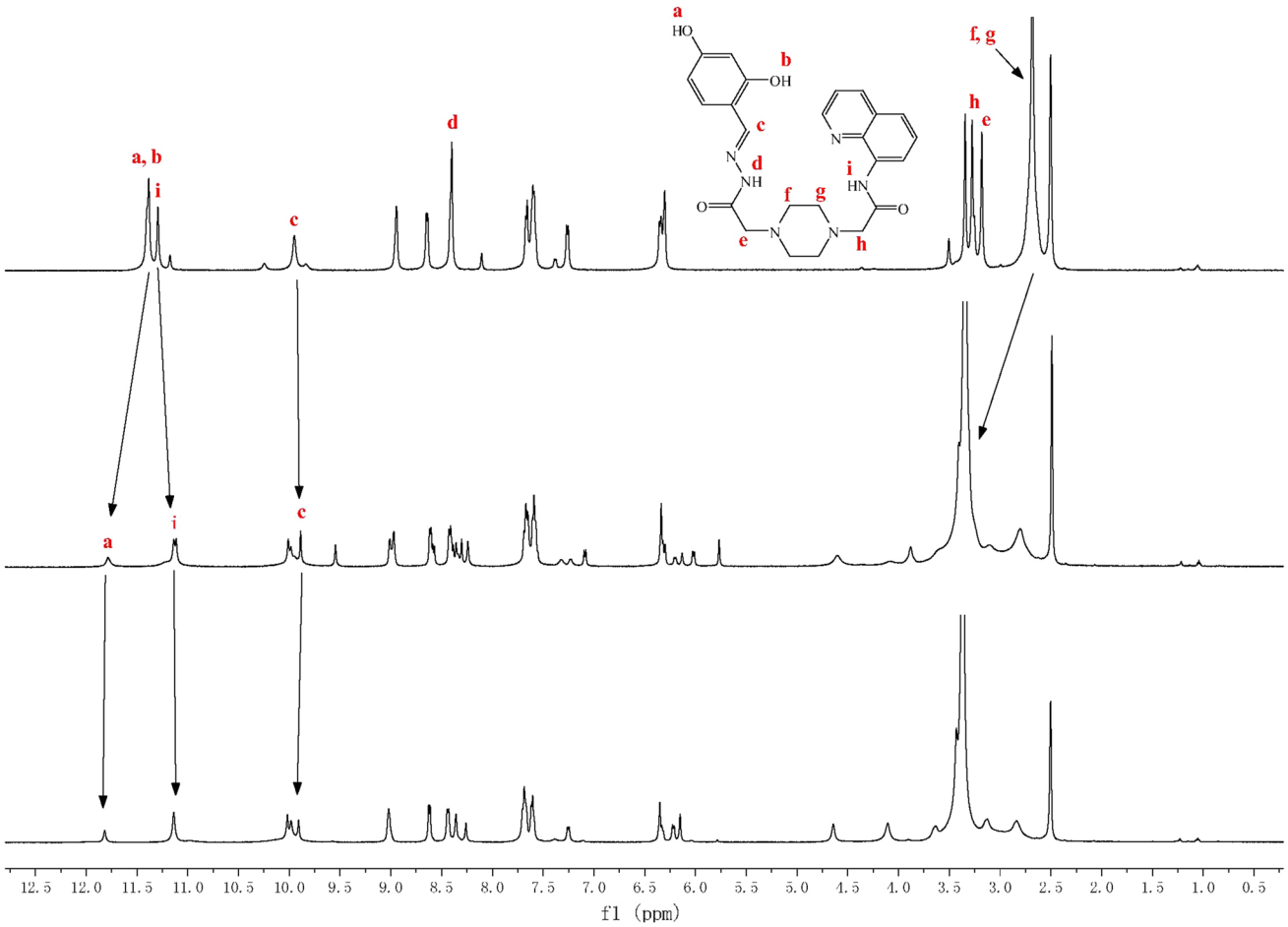

Fig. 9 ^{1}H NMR spectra of BQPA with Al^{3+} in DMSO-d_6

Table 1 Comparison of BQPA with previously reported probes for Al^{3+} ions

Mechanism	Selectivity	Linear range (μM)	Solution (v/v)	LOD (μM)	Increased intensity by Al^{3+} (times)	References
ICT	Al^{3+}	3–7	EtOH–H_2O (2:3)	0.0578	11	Singh et al. (2017)
CHEF	Al^{3+}	0–10	EtOH–H_2O (4:1)	0.299	20	Gan et al. (2017)
ESIPT	Al^{3+}	0–0.01	EtOH–H_2O (1:5)	0.00812	20	Balakrishnan et al. (2017)
hydrolysis	Al^{3+}, Cu^{2+}	0–10	EtOH-H_2O (6:4)	4.369	2	Zhang et al. (2018)
RET	Se, Te	NR	EtOH–H_2O (2:3)	1.0	NR	Manjare et al. (2014)
PET	Al^{3+}	3–11	DMF–H_2O (1:1)	0.034	8	Wang et al. (2017a, b
ESIPT, CHEF	Al^{3+}, F^{-}	0–3	EtOH	0.924	200	Lim et al. (2018)
AIE	Al^{3+}, ppi	0–180	DMF–H_2O (5:1)	0.39	35	Wang et al. (2018a, b, c)
CHEF	Al^{3+}, Fe^{3+}	3.33–33.3	DMSO–H_2O (1:1)	0.358	20	Dai et al. (2018)
FRET	Al^{3+}	0–20	H_2O	NR	400	Maniyazagan et al. (2018)
CHEF	Al^{3+}	2–12	EtOH–H_2O (1:9)	0.031	300	Present work

LOD the limit of detection, *NR* not reported in the corresponding paper

and the corresponding fluorescence spectrum tested (Fig. S11–13). The results showed that when the concentration of Cu^{2+} was lower than 0.2 μM, the accuracy in the detection of Al^{3+} was almost unaffected. This result indicated that BQPA could be used for Al^{3+} detection in water samples even with the co-existence of trace Cu^{2+}.

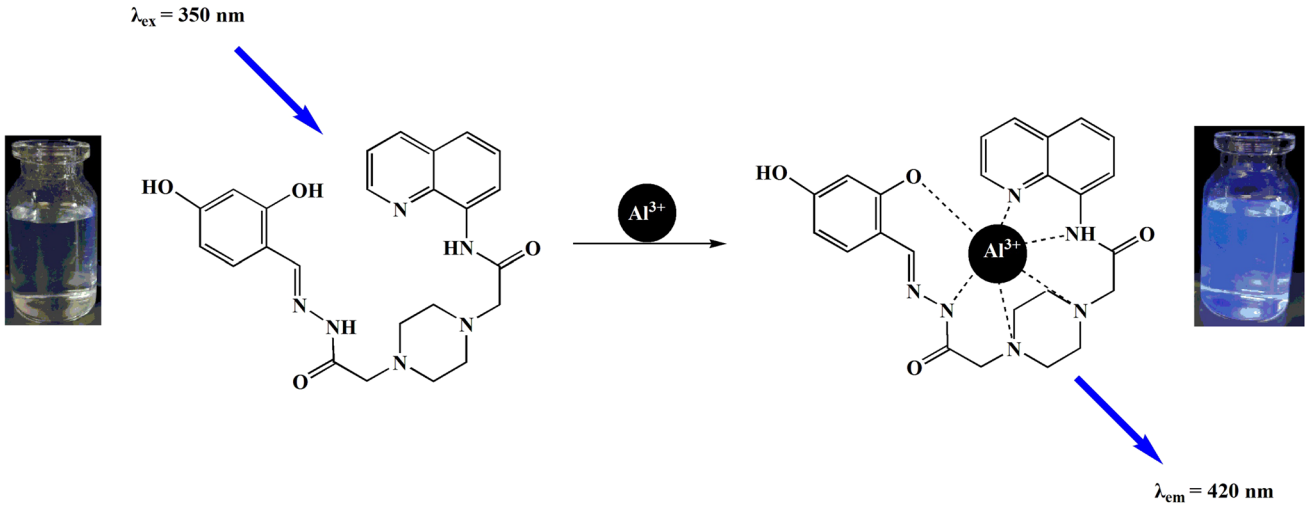

Scheme 2 Proposed binding mode of BQPA with Al^{3+}

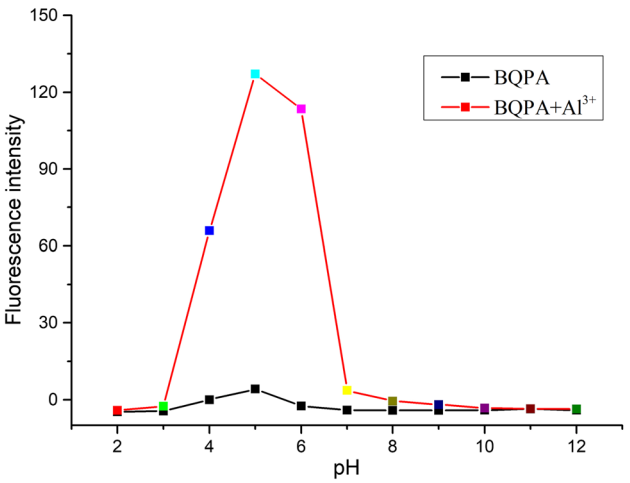

Fig. 10 The variation in fluorescence intensity with the pH of BQPA in the presence of Al^{3+} (5.0 eq.) at 420 nm

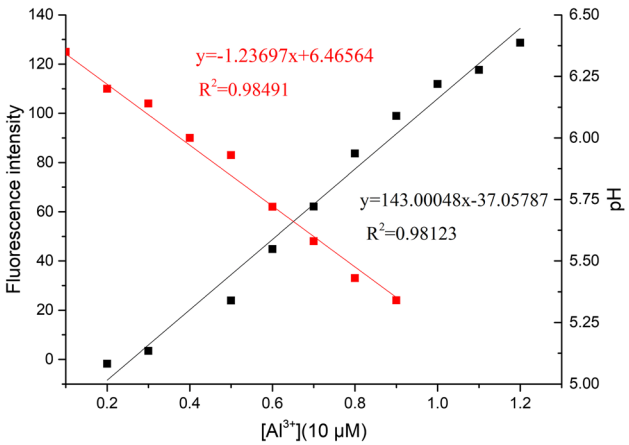

Fig. 11 The relationship of fluorescence intensity (black, λ_{em} = 420 nm) and pH (red) with different concentrations of Al^{3+} in ethanol/water (1:9, v/v)

Conclusions

In summary, a novel fluorescent chemosensor BQPA was synthesized and characterized based on quinoline derivative. It showed significant fluorescence enhancement (300-fold) accompanied by color change from colorless to blue, and ratiometric absorbance for the highly sensitive detection of Al^{3+} in ethanol/water (1:9, v/v). The 1:1 stoichiometry of the BQPA–Al^{3+} complexes was determined, and the detection limits of probe BQPA for Al^{3+} was 31 nM, which was sensitive enough to detect Al^{3+} in water samples.

Acknowledgements This work was supported by the Research Science Foundation in Technology Innovation of Harbin (no. 2017RAQXJ022) and the Postdoctoral Scientific Research Developmental Fund of Heilongjiang Province (no. LBH-Q14023). We would like to thank Zhe Wang (Qiqihar University) for the MS measurement.

References

Balakrishnan C, Neelakantan MA, Banerjee S (2017) A zwitterionic pH responsive ESIPT-Based fluorescence "Turn-On" Al^{3+} ion sensing probe and its bioimaging applications. Sens Actuators B Chem 253:1012–1025. https://doi.org/10.1016/j.snb.2017.07.030

Carter KP, Young AM, Palmer AE (2014) Fluorescent sensors for measuring metal ions in living systems. Chem Rev 114:4564–4601. https://doi.org/10.1021/cr400546e

Chen TT, Yin LY, Huang CS, Qin YQ, Zhu WP, Xu YF, Qian XH (2015) Highly selective "Off–On" fluorescent probe for histidine and its imaging in living cells. Biosens Bioelectron 66:259–265. https://doi.org/10.1016/j.bios.2014.11.005

Table 2 Determination of BQPA for Al^{3+} in tap water and ultrapure water

Water samples studied	Amount of standard Al^{3+} added (μM)	Total Al^{3+} found ($n=3$) (μM)	Recovery of Al^{3+} ($n=3$) added (%)	RSD (%)	Relative error (%)
Ultrapure water	6	5.73	95.55	5.90	−5.00
	7	6.78	96.86	5.10	−2.86
	8	8.13	101.63	2.84	1.63
Tap water (Department of Chemistry)	6	5.78	96.33	4.60	−3.67
	7	6.71	95.86	3.53	−4.14
	8	8.19	102.38	1.75	2.38

Chitnis SD, Akhlaghi F (2008) Development and validation of an HPLC-UV method for iodixanol quantification in human plasma. J Chromatogr B 869:133–137. https://doi.org/10.1016/j.jchromb.2008.05.002

Dai YP, Fu JX, Yao K, Song QQ, Xu KX, Pang XB (2018) A novel turn-on fluorescent probe for Al^{3+} and Fe^{3+} in aqueous solution and its imaging in living cells. Spectrochim Acta A Mol Biomol Spectrosc 192:257–262. https://doi.org/10.1016/j.saa.2017.11.001

Fan L, Qin J, Li T, Wu Z, Wang B, Yang Z (2014) A chromone Schiff-base as Al(III) selective fluorescent and colorimetric chemosensor. J Lumin 155:84–88. https://doi.org/10.1016/j.jlumin.2014.06.023

Fu Y, Pang XX, Wang ZQ, Chai Q, Ye F (2019) A highly sensitive and selective fluorescent probe for determination of Cu(II) and application in live cell imaging. Spectrochim Acta A Mol Biomol Spectrosc 208:198–205. https://doi.org/10.1016/j.saa.2018.10.005

Gan XP, Li W, Li CX, Wu ZC, Liu D, Huang B, Zhou HP, Tian YP (2017) Two analogously structural triphenylamine-based fluorescent "off-on" probes for Al^{3+} via two distinct mechanisms and cell imaging application. Sens Actuators B Chem 239:642–651. https://doi.org/10.1016/j.snb.2016.08.042

Good PF, Olanow CW, Perl DP (1992) Neuromelanin-containing neurons of the substantia nigra accumulate iron and aluminum in Parkinson's disease: a LAMMA study. Brain Res 593:343–346. https://doi.org/10.1016/0006-8993(92)91334-b

Gupta N, Kaur T, Bhalla V, Parihar RD, Ohri P, Kaur G, Kumar M (2017) A naphthalimide-based solid state luminescent probe for ratiometric detection of aluminum ions: in vitro and in vivo applications. Chem Commun 53:12646–12649. https://doi.org/10.1039/c7cc07996f

Han T, Feng X, Tong B, Shi J, Chen L, Zhi J, Dong Y (2012) A novel "turn-on" fluorescent chemosensor for the selective detection of Al^{3+} based on aggregation-induced emission. Chem Commun 48:416–418. https://doi.org/10.1039/c1cc15681k

Hosseinzadeh R, Mohadjerani M, Pooryousef M, Eslami A, Emami S (2015) A new boronic acid fluorescent sensor based on fluorene for monosaccharides at physiological pH. Spectrochim Acta A Mol Biomol Spectrosc 144:53–60. https://doi.org/10.1016/j.saa.2015.02.066

Huang SS, Li FF, Liao CY, Zheng BZ, Du J, Xiao D (2017) A selective and sensitive fluorescent probe for the determination of HSA and trypsin. Talanta 170:562–568. https://doi.org/10.1016/j.talanta.2017.01.034

Kadar M, Biro A, Toth K, Vermes B, Huszthy P (2005) Spectrophotometric determination of the dissociation constants of crown ethers with grafted acridone unit in methanol based on Benesi-Hildebrand evaluation. Spectrochim Acta A Mol Biomol Spectrosc 62:1032–1038. https://doi.org/10.1016/j.saa.2005.04.034

Kang L, Xing ZY, Ma XY, Liu YT, Zhang Y (2016) A highly selective colorimetric and fluorescent turn-on chemosensor for Al^{3+} based on naphthalimide derivative. Spectrochim Acta A Mol Biomol Spectrosc 167:59–65. https://doi.org/10.1016/j.saa.2016.05.030

Kumawat LK, Mergu N, Asif M, Gupta VK (2016) Novel synthesized antipyrine derivative based "Naked eye" colorimetric chemosensors for Al^{3+} and Cr^{3+}. Sens Actuators B Chem 231:847–859. https://doi.org/10.1016/j.snb.2016.03.062

Li JF, Yin CX, Huo FJ (2016) Development of fluorescent zinc chemosensors based on various fluorophores and their applications in zinc recognition. Dyes Pigments 131:100–133. https://doi.org/10.1016/j.dyepig.2016.03.043

Li Z, Wang S, Xiao L, Li X, Shao X, Jing X, Peng X, Ren L (2018) An efficient colorimetric probe for fluoride ion based on schiff base. Inorg Chim Acta 476:7–11. https://doi.org/10.1016/j.ica.2018.01.011

Lim C, Seo H, Choi JH, Kim KS, Helal A, Kim HK (2018) Highly selective fluorescent probe for switch-on Al^{3+} detection and switch-off F^- detection. J Photochem Photobiol A 356:312–320. https://doi.org/10.1016/j.jphotochem.2018.01.012

Liu Y, Xiang K, Guo M, Tian B, Zhang J (2016) A coumarin-based fluorescent probe for the fast detection of Pd^0 with low detection limit. Tetrahedron Lett 57:1451–1455. https://doi.org/10.1016/j.tetlet.2016.02.062

Maniyazagan M, Mariadasse R, Nachiappan M, Jeyakanthan J, Lokanath NK, Naveen S, Sivaraman G, Muthuraja P, Manisankar P, Stalin T (2018) Synthesis of rhodamine based organic nanorods for efficient chemosensor probe for Al(III) ions and its biological applications. Sens Actuators B Chem 254:795–804. https://doi.org/10.1016/j.snb.2017.07.106

Manjare ST, Kim Y, Churchill DG (2014) Selenium- and tellurium-containing fluorescent molecular probes for the detection of biologically important analytes. Acc Chem Res 47:2985–2998. https://doi.org/10.1021/ar500187v

Manna A, Sain D, Guchhait N, Goswami S (2017) FRET based selective and ratiometric detection of Al(III) with live-cell imaging. New J Chem 41:14266–14271. https://doi.org/10.1039/c7nj03079g

More P, Shankarling GS (2017) Reversible "turn off" fluorescence response of Cu^{2+} ions towards 2-pyridyl quinoline based chemosensor with visible colour change. Sens Actuators B Chem 241:552–559. https://doi.org/10.1016/j.aca.2016.09.036

Naskar B, Das K, Mondal RR, Maiti DK, Requena A, Cerón-Carrasco JP, Prodhan C, Chaudhuri K, Goswami S (2018) A new fluorescence turn-on chemosensor for nanomolar detection of Al^{3+} constructed from a pyridine–pyrazole system. New J Chem 42:2933–2941. https://doi.org/10.1039/c7nj03955g

Nie J, Li N, Ni Z, Zhao Y, Zhang L (2017) A sensitive tetraphenylethene-based fluorescent probe for Zn^{2+} ion involving ESIPT and CHEF processes. Tetrahedron Lett 58:1980–1984. https://doi.org/10.1016/j.tetlet.2017.04.027

Okem A, Southway C, Stirk WA, Street RA, Finnie JF, Staden JV (2015) Effect of cadmium and aluminum on growth, metabolite content and biological activity in *Drimia elata*

(Jacq.) Hyacinthaceae. S Afr J Bot 98:142–147. https://doi.org/10.1016/j.sajb.2015.02.013
Öksüza N, Saçmac Ş, Saçmac M, Ülgen A (2019) A new fluorescence reagent: synthesis, characterization and application for speciation of arsenic (III)/(VI) species in tea samples. Food Chem 270:579–584. https://doi.org/10.1016/j.foodchem.2018.07.076
Özyol E, Saçmac Ş, Saçmac M, Ülgen A (2018) A new turn-on fluorimetric method for the rapid speciation of Cr(III)/Cr(VI) species in tea samples with rhodamine-based fluorescent reagent. Spectrochim Acta A Mol Biomol Spectrosc 191:62–68. https://doi.org/10.1016/j.saa.2017.10.005
Pang B, Li C, Yang Z (2018) Design of a colorimetric and turn-on fluorescent probe for the detection of Al(III). J Photochem Photobiol A 356:159–165. https://doi.org/10.1016/j.jphotochem.2017.12.046
Qin JC, Yang ZY (2015a) Selective fluorescent sensor for Al^{3+} using a novel quinoline derivative in aqueous solution. Synth Met 209:570–576. https://doi.org/10.1016/j.synthmet.2015.09.021
Qin JC, Yang ZY (2015b) Ratiometric fluorescent probe for Al^{3+} based on coumarin derivative in aqueous media. Anal Methods 7:2036–2040. https://doi.org/10.1039/c4ay02971b
Ren XJ, Tian HH, Yang L, He L, Geng YN, Liu XJ, Song XZ (2018) Fluorescent probe for simultaneous discrimination of Cys/Hcy and GSH in pure aqueous media with a fast response under a single-wavelength excitation. Sens Actuators B Chem 273:1170–1178. https://doi.org/10.1016/j.snb.2018.04.163
Roy SB, Rajak KK (2017) A quinoline appended naphthalene derivative based AIE active "turn–on" fluorescent probe for the selective recognition of Al^{3+} and colourimetric sensor for Cu^{2+}: experimental and computational studies. J Photochem Photobiol A 332:505–514. https://doi.org/10.1016/j.jphotochem.2016.09.015
Roy A, Dey S, Roy P (2016) A ratiometric chemosensor for Al^{3+} based on naphthalene-quinoline conjugate with the resultant complex as secondary sensor for F^{-}: interpretation of molecular logic gates. Sens Actuators B Chem 237:628–642. https://doi.org/10.1016/j.snb.2016.06.139
Saçmaci Ş, Saçmaci M, Ülgen A (2017) A new turn-on fluorometric detection method for the determination of Ag(I) in some food and water samples. J AOAC Int 100:1854–1860. https://doi.org/10.5740/jaoacint.17-0090
Shao J (2010) A novel colorimetric and fluorescence anion sensor with a urea group as binding site and a coumarin group as signal unit. Dyes Pigments 87:272–276. https://doi.org/10.1016/j.dyepig.2010.04.007
Shyamal M, Mazumdar P, Maity S, Sahoo GP, Morán GS, Misra A (2016) Pyrene scaffold as real-Time fluorescent turn-on chemosensor for selective detection of trace-level Al(III) and its aggregation-induced emission enhancement. J Phys Chem A 120:210–220. https://doi.org/10.1021/acs.jpca.5b09107
Singh DP, Dwivedi R, Singh AK, Kochc B, Singh P, Singh VP (2017) A dihydrazone based "turn-on" fluorescent probe for selective determination of Al^{3+} ions in aqueous ethanol. Sens Actuators B Chem 238:128–137. https://doi.org/10.1016/j.snb.2016.07.043
Singh R, Samanta S, Mullick P, Ramesh A, Das G (2018) Al^{3+} sensing through different turn-on emission signals vis-à-vis two different excitations: applications in biological and environmental realms. Anal Chim Acta 1025:172–180. https://doi.org/10.1016/j.aca.2018.03.053
Walton JR (2007) An aluminum-based rat model for Alzheimer's disease exhibits oxidative damage, inhibition of PP2A activity, hyperphosphorylated tau, and granulovacuolar degeneration. J Inorg Biochem 101:1275–1284. https://doi.org/10.1016/j.jinorgbio.2007.06.001
Wang GQ, Qin JC, Li CR, Yang ZY (2015a) A highly selective fluorescent probe for Al^{3+} based on quinoline derivative. Spectrochim Acta A Mol Biomol Spectrosc 150:21–25. https://doi.org/10.1016/j.saa.2015.05.041
Wang XJ, Feng LH, Zhang LW (2015b) Construction and application of a facile chemosensor for monosaccharides detection in blood and urine. Sens Actuators B Chem 208:588–592. https://doi.org/10.1016/j.snb.2014.11.095
Wang F, Xu YL, Aderinto SO, Peng HP, Zhang H, Wu HL (2017a) A new highly effective fluorescent probe for Al^{3+} ions and its application in practical samples. J Photochem Photobiol A 332:273–282. https://doi.org/10.1016/j.jphotochem.2016.09.004
Wang Z, Wu Q, Li J, Qiu S, Cao D, Xu Y, Liu Z, Yu X, Sun Y (2017b) Two benzoyl coumarin amide fluorescence chemosensors for cyanide anions. Spectrochim Acta A Mol Biomol Spectrosc 183:1–6. https://doi.org/10.1016/j.saa.2017.04.008
Wang CJ, Xia X, Luo JR, Qian Y (2018a) A novel near-infrared styryl-BODIPY fluorescent probe for discrimination of GSH and its application in living cells. Dyes Pigments 152:85–92. https://doi.org/10.1016/j.dyepig.2018.01.034
Wang Q, Wen XY, Fan ZF (2018b) A Schiff base fluorescent chemosensor for the double detection of Al^{3+} and PPi through aggregation induced emission in environmental physiology. J Photochem Photobiol A 358:92–99. https://doi.org/10.1016/j.jphotochem.2018.03.004
Wang Y, Wang LJ, Jiang EK, Zhu MQ, Wang Z, Fan SS, Gao Q, Liu SZ, Li QX, Hua RM (2018c) A colorimetric and ratiometric dual-site fluorescent probe with 2,4-dinitrobenzenesulfonyl and aldehyde groups for imaging of aminothiols in living cells and zebrafish. Dyes Pigments 156:338–347. https://doi.org/10.1016/j.dyepig.2018.04.027
Wen X, Fan Z (2016) Linear Schiff-base fluorescence probe with aggregation-induced emission characteristics for Al^{3+} detection and its application in live cell imaging. Anal Chim Acta 945:75–84. https://doi.org/10.1016/j.aca.2016.09.036
Yıldız E, Saçmac S, Saçmac M, Ülgen A (2017) Synthesis, characterization and application of a new fluorescence reagent for the determination of aluminum in food samples. Food Chem 237:942–947. https://doi.org/10.1016/j.foodchem.2017.06.055
Zeng S, Li SJ, Sun XJ, Li MQ, Ma YQ, Xing ZY, Li JL (2018) A naphthalene-quinoline based chemosensor for fluorescent "turn-on"and absorbance-ratiometric detection of Al^{3+} and its application in cells imaging. Spectrochim Acta A Mol Biomol Spectrosc 205:276–286. https://doi.org/10.1016/j.saa.2018.07.039
Zhang X, Sun P, Li F, Li H, Zhou HP, Wang H, Zhang BW, Pan ZW, Tian YP, Zhang XJ (2018) A tissue-permeable fluorescent probe for Al(III), Cu(II) imaging in vivo. Sens Actuators B Chem 255:366–373. https://doi.org/10.1016/j.snb.2017.07.196
Zhou F, Wang H, Liu P, Hu Q, Wang Y, Liu C, Hu J (2018) A highly selective and sensitive turn-on probe for aluminum(III) based on quinoline Schiff's base and its cell imaging. Spectrochim Acta A Mol Biomol Spectrosc 190:104–110. https://doi.org/10.1016/j.saa.2017.09.007
Zhu Q, Li L, Mu L, Zeng X, Carl Redshaw, Wei G (2016) A ratiometric Al^{3+} ion probe based on the coumarin-quinoline FRET system. J Photochem Photobiol A 328:217–224. https://doi.org/10.1016/j.jphotochem.2016.06.006